

Protease-activated receptor-3 (PAR3) regulates PAR1 signaling by receptor dimerization

Joseph N. McLaughlin, Myla M. Patterson, and Asrar B. Malik

PNAS 2007;104;5662-5667; originally published online Mar 21, 2007;
doi:10.1073/pnas.0700763104

This information is current as of April 2007.

| | |
|--|---|
| Online Information & Services | High-resolution figures, a citation map, links to PubMed and Google Scholar, etc., can be found at: www.pnas.org/cgi/content/full/104/13/5662 |
| Supplementary Material | Supplementary material can be found at: www.pnas.org/cgi/content/full/0700763104/DC1 |
| References | This article cites 37 articles, 17 of which you can access for free at: www.pnas.org/cgi/content/full/104/13/5662#BIBL This article has been cited by other articles: www.pnas.org/cgi/content/full/104/13/5662#otherarticles |
| E-mail Alerts | Receive free email alerts when new articles cite this article - sign up in the box at the top right corner of the article or click here . |
| Rights & Permissions | To reproduce this article in part (figures, tables) or in entirety, see: www.pnas.org/misc/rightperm.shtml |
| Reprints | To order reprints, see: www.pnas.org/misc/reprints.shtml |

Notes:

Protease-activated receptor-3 (PAR3) regulates PAR1 signaling by receptor dimerization

Joseph N. McLaughlin*, Myla M. Patterson, and Asrar B. Malik

Department of Pharmacology and Center for Lung and Vascular Biology, University of Illinois College of Medicine, Chicago, IL 60612

Communicated by Ivar Giaever, Applied BioPhysics, Inc., Troy, NY, February 7, 2007 (received for review November 3, 2006)

Thrombin activates endothelial cell signaling by cleaving the protease-activated receptor-1 (PAR1). However, the function of the apparently nonsignaling receptor PAR3 also expressed in endothelial cells is unknown. We demonstrate here the crucial role of PAR3 in potentiating the responsiveness of PAR1 to thrombin. We tested the hypothesis that PAR1/PAR3 heterodimerization and its effect in modifying G protein selectivity was responsible for PAR3 regulation of PAR1 sensitivity. Using bioluminescent resonance energy transfer-2, we showed that PAR1 had comparable dimerization affinity for PAR3 as for itself. We observed increased $G\alpha_{13}$ coupling between the PAR1/3 heterodimer compared with the PAR1/1 homodimer. Moreover, knockdown of PAR3 moderated the PAR1-activated increase in endothelial permeability. These results demonstrate a role of PAR3 in allosterically regulating PAR1 signaling governing increased endothelial permeability. Because PAR3 is a critical determinant of PAR1 function, targeting of PAR3 may mitigate the effects of PAR1 in activating endothelial responses such as vascular inflammation.

signal transduction | thrombin | endothelium | functional selectivity | G protein

Thrombin generation during thrombosis contributes to the pathophysiology of multiple thrombosis-related diseases such as acute lung injury resulting increased endothelial permeability (1), vascular inflammation (1, 2), and edema formation (for recent reviews, see refs. 3 and 4). These complications are the result of thrombin activation of protease-activated receptor-1 (PAR1) (5). Cleavage of the extracellular N terminus of PAR1 initiates signaling (6) by the concomitant activation of heterotrimeric GTP-binding proteins $G\alpha_q$ and $G\alpha_{12/13}$ (7–9). The mechanisms by which PAR1 selectively activates G protein signaling remain unknown. Because the nonsignaling receptor PAR3 is also expressed in endothelial cells (10), we surmised that PAR1 and PAR3 are capable of interacting in such manner as to regulate PAR1 signaling. We found that PAR3 directly dimerizes with PAR1 to induce a specific PAR1/ $G\alpha_{13}$ -binding conformation that favors $G\alpha_{13}$ activation. We propose a model of PAR1 activation involving the interaction with PAR3, which alters the selectivity of PAR1 for $G\alpha_{13}$ coupling and promotes endothelial barrier dysfunction. PAR3 functions as an essential allosteric modulator of PAR1 signaling through PAR1/3 dimerization and favors a distinct $G\alpha_{13}$ -activated downstream pathway.

Results

PAR3 Knockdown in Endothelial Cells Shifts the Potency of Thrombin Activation of PAR1. Endothelial cells express PAR1, -2, and -3, but not PAR4 (10), and of these only PAR1 and PAR3 are thrombin-sensitive (11). To address whether PAR3 alters thrombin signaling in endothelial cells, siRNA knockdown was used to reduce thrombin receptor expression in human pulmonary artery endothelial cells (HPAECs). PAR1 and PAR3 suppression was determined by semiquantitative RT-PCR. siRNA against PAR3 did not affect PAR1 expression, whereas it reduced PAR3 expression 8-fold. Conversely, siRNA against PAR1 only modestly affected PAR3 expression, whereas it suppressed PAR1

expression 9-fold [supporting information (SI) Fig. 6]. We next determined the effects of altered receptor expression by using two functional outputs: (i) intracellular calcium mobilization ($[Ca^{2+}]_i$) and (ii) endothelial barrier dysfunction. Thrombin-induced (0.1–10.0 nM) increase in $[Ca^{2+}]_i$ was assessed in knockdown HPAECs. PAR1 knockdown showed a marked reduction in maximal peak height, whereas PAR3 knockdown did not (Fig. 1A). The lack of effect of PAR3 siRNA on $[Ca^{2+}]_i$ was used to control for nonspecific effects of siRNA treatment. Dose–response curves (Fig. 1C) of maximum peak height yielded the following EC_{50} values and corresponding 95% confidence intervals: control = 0.18 nM (0.04–0.8), siRNA PAR3 = 0.13 nM (0.06–0.4), and siRNA PAR1 = 1.5 nM (0.2–11.1). PAR3 knockdown showed no statistically significant difference in $[Ca^{2+}]_i$, whereas PAR1 knockdown altered both thrombin potency and efficacy, thus indicating the efficacy of PAR1 siRNA treatment.

We next addressed the effects of PAR1 or PAR3 knockdown on endothelial barrier function. Thrombin-induced (1–100 nM) transendothelial electrical resistance (TER) was assayed in knockdown HPAECs. PAR1 knockdown showed virtually no responsiveness at 10 nM thrombin compared with controls, whereas PAR3 knockdown reduced the response by 50% (Fig. 1B). Dose–response curves (Fig. 1D) of the minimal-induced TER yielded the following EC_{50} with 95% confidence intervals: control = 5.5 nM (4.1–7.5), siRNA PAR3 = 15.3 nM (8.0–29.4), and siRNA PAR1 = 80.9 nM (38.8–169). PAR3 knockdown showed a modest difference in thrombin-induced endothelial barrier dysfunction, whereas PAR1 knockdown markedly altered both thrombin potency and efficacy.

PAR1 and PAR3 Form Constitutive Heterodimers. To address the mechanism of how down-regulation of PAR3 affects PAR1 signaling, we investigated interactions between PAR1 and PAR3 by using bioluminescent resonance energy transfer-2 (BRET²) (12–15). Using BRET² PAR dimerization was assessed by transient expression of pairs of C-terminally tagged fusion proteins, one receptor tagged with *Renilla* luciferase (Rluc) and the other with modified GFP-2 (GFP²), followed by the addition of the cell permeable luciferase substrate and subsequent measurement of emission ratio (510/410 nm). Specific receptor/receptor interactions are characterized by a hyperbolic increase in BRET² signal as the ratio of receptor-GFP² to receptor-Rluc

Author contributions: J.N.M. designed research; J.N.M. and M.M.P. performed research; A.B.M. contributed new reagents/analytic tools; J.N.M. analyzed data; and J.N.M. and A.B.M. wrote the paper.

The authors declare no conflict of interest.

Abbreviations: BRET², bioluminescent resonance energy transfer-2; EBM-2, endothelial growth medium-2; GFP², modified GFP; GPCR, G-protein coupled receptor; HPAEC, human pulmonary artery endothelial cells; PAR, protease-activated receptor; Rluc, *Renilla* luciferase; T39P, thrombin-insensitive mutant of PAR3; TER, transendothelial electrical resistance; TK, PAR1-specific agonist peptide TFLLRNPNDK.

*To whom correspondence should be addressed. E-mail: mclaugh1@uic.edu.

This article contains supporting information online at www.pnas.org/cgi/content/full/0700763104/DC1.

© 2007 by The National Academy of Sciences of the USA

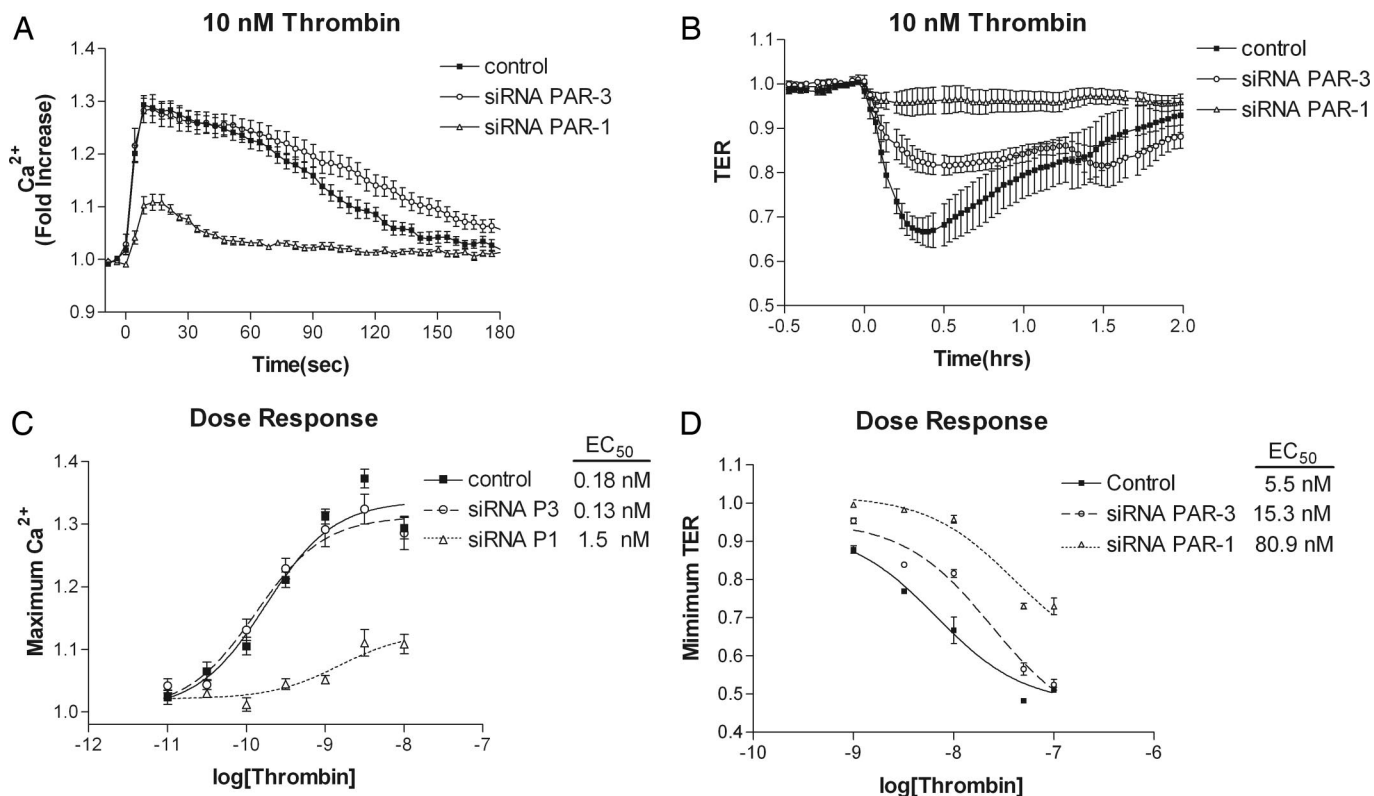


Fig. 1. Differential effects of PAR1 and PAR3 siRNA knockdown in endothelial cells on thrombin-induced mobilization of intracellular calcium and thrombin-induced increase of endothelial monolayer permeability. Cultured HPAECs were electroporated with either buffer alone (control) or pools of siRNA specific for PAR3 or PAR1. (A) Resultant intracellular calcium mobilization traces for each knockdown and control group at a representative thrombin concentration of 10 nM. (B) Changes in endothelial monolayer permeability (TER) determined at a representative thrombin concentration of 10 nM. (C) Dose–response curves of the maximal-induced calcium response for each group. (D) Dose–response curves of the minimal-induced TER for each group. Each point represents the average of at least three separate experiments performed in duplicate. Error bars represent \pm SEM.

expression increases (16). Nonspecific interactions, conversely, increase in direct proportion to the acceptor:donor ratio and give a linear increase in BRET² signal.

We cotransfected human embryonic kidney (HEK)293T cells with a fixed amount of PAR1-Rluc cDNA (0.5 μ g) and increasing amounts (0.5, 1.0, 1.5, 2.0, and 2.5 μ g) of GABABR2-GFP² (as nonspecific control) or PAR1-GFP² cDNA. The BRET² signal and the GFP²/Rluc ratio were quantitatively determined as described in *Materials and Methods*.

The nonspecific signal from the PAR1-Rluc/GABABR2-GFP² interaction exhibited a small but linear increase, whereas PAR1-Rluc/PAR1-GFP² exhibited a substantial and hyperbolic increase in signal (Fig. 2A). Similar results were observed for the PAR1/3 heterodimer and PAR3/3 homodimer. Thus, the dimerization of PARs is highly specific and not the result per se of overexpression or saturation of the signal. To ensure the BRET² signal was originating from properly localized receptors, plasma membrane localization of PAR1-GFP² was determined by using standard fluorescent confocal microscopy (Fig. 2B). The corresponding PAR1-Rluc was visualized in the same cells by immunohistochemistry by using a primary antibody against Rluc and a fluorescent-conjugated secondary antibody (Fig. 2C). We observed that corresponding PAR3 constructs showed a similar subcellular localization (data not shown).

In addition to assessing PAR interactions, BRET² was used to determine the relative binding affinities between the different partners (16). The rate at which the BRET² signal is saturated as the GFP²/Rluc ratio is increased depends on the relative binding affinities of the two molecules (16). The value of the GFP²/Rluc ratio at 50% maximum NetBRET², or BRET₅₀ is an

estimate of the relative affinities of the receptors for each other and follows the K_d value; i.e., a lower BRET₅₀ would indicate greater affinity. The following BRET₅₀ values with 95% confidence intervals were obtained from data in Fig. 2A. PAR1/1 = 0.093 (0.05–0.13), PAR3/3 = 0.036 (0.001–0.071), and PAR1/3 = 0.036 (0.032–0.039).

Effects of PAR1 Activation After Dimerization with PAR3. We next determined the effects of activation of PAR1 on its dimerization state with PAR3. We used thrombin as well as the PAR1-specific agonist peptide TFLLRNPNDK (TK). PAR1-Rluc was transiently coexpressed in HEK293T cells with either PAR1-GFP² or PAR3-GFP² at the optimal GFP²/Rluc ratio determined (as shown in Fig. 2). Cells were treated with 10 nM thrombin or 100 μ M TK, and the BRET² signal was immediately (time = 0) measured or measured after 30 min. The BRET² signal was not initially affected by receptor activation induced by thrombin or TK for either PAR1/1 or PAR1/3. However, after 30 min, activation by thrombin produced 50% decrease in signal for both the PAR1/1 homodimer and PAR1/3 heterodimer. Importantly, 30-min activation with TK caused a decrease in signal only for the PAR1/3 heterodimer; PAR1/1 homodimer was unaffected (Fig. 3).

PAR Dimer Constitution Regulates G Protein Selectivity. We next addressed the effects of receptor dimerization on $G\alpha_q$ and $G\alpha_{13}$ G protein selectivity by using receptors tagged with Rluc and G protein tagged with GFP². Specific receptor dimer expression was accomplished by cotransfection of 0.5 μ g of PAR1-Rluc plasmid DNA into HEK293T cells with either 1.0 μ g of untagged PAR1 or untagged PAR3 plasmid DNA. Coexpression of the

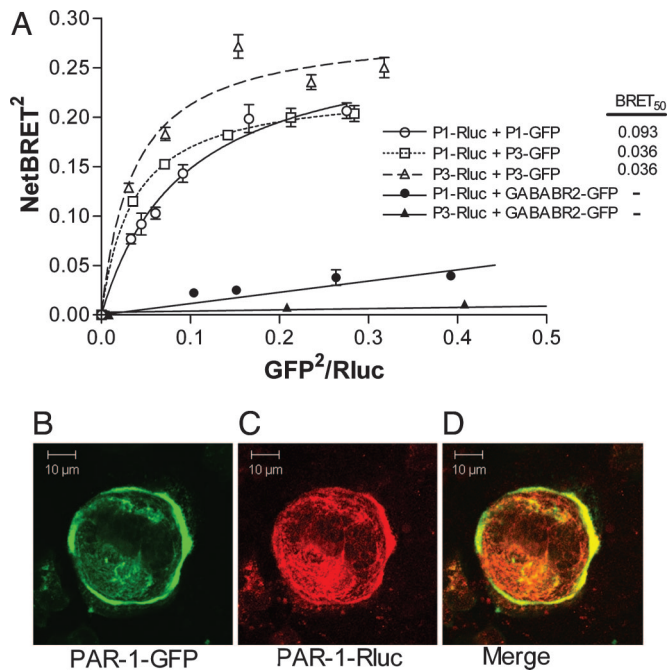


Fig. 2. Specificity and localization of PAR1/PAR3 homo- and heterodimers. A constant amount PAR1- or PAR3-Rluc cDNA was transiently transfected into HEK293T cells along with increasing amounts of PAR1-GFP², PAR3-GFP² or GABABR2-GFP² cDNA. (A) Total Rluc, GFP, and BRET² signals were determined as described in *Materials and Methods*. Each point represents the average of at least three separate experiments performed in duplicate. Error bars represent \pm SEM. (B) A representative image of PAR1-GFP² plasma membrane localization by fluorescent microscopy (green). (C) Rluc constructs were visualized in the same cells by immunohistochemistry using a primary antibody against Rluc and a fluorescent-conjugated secondary antibody (red). (D) Co-localization (merge) at the plasma membrane (yellow).

untagged form of either PAR1 or PAR3 with labeled PAR1 would ensure that the BRET² signal would originate only from the PAR1 subunit of the complex.

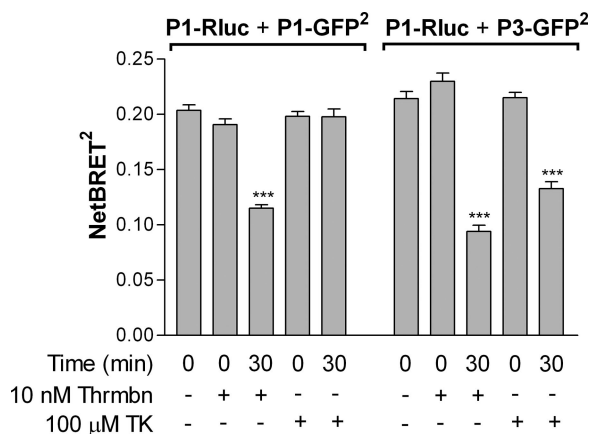


Fig. 3. Effects of agonist-induced receptor activation on BRET² signal resulting from receptor dimerization. PAR1-Rluc was transiently coexpressed in HEK293T cells with either PAR1-GFP² or PAR3-GFP², as indicated. Cells were stimulated with either 10 nM thrombin or 100 μM TK, after which BRET² signal was determined immediately (time, 0 min), then again after 30 min. We report here differences between PAR1/1 and PAR1/3 dimer pairs in response to agonist peptide at 30 min, although we observed the same trend within 5 min after activation (data not shown). Each bar represents the average of at least three separate experiments performed in duplicate. Error bars represent \pm SEM. ***, $P < 0.0001$.

GFP²-labeled G proteins were introduced by two methods of cotransfecting 1.0 μg each of either (i) nontagged G α -subunit, G β ₁ tagged on the N terminus with GFP² (GFP²-G β ₁) and nontagged G γ ₂ or (ii) internally tagged GFP²-G α -subunit, nontagged G β ₁, and nontagged G γ ₂.

When labeled on the N terminus, GFP²-G β ₁ is fully capable of G protein-coupled receptor (GPCR) coupling and signaling (13). In the case of the α subunit of G α _q and G α ₁₃, the GFP² cannot be attached at either terminus, because it interferes with GPCR coupling. Instead, the GFP moiety was incorporated internally. Following a precedent for G α _q in which insertion between amino acids E119 and N120 yielded functional protein (17), for G α ₁₃, GFP² was inserted between amino acids P130 and M131. All of the fluorescent G protein constructs were expressed in HEK293T cells and found to localize to the plasma membrane (data not shown).

Because the ability of GFP²-G β ₁ to couple to receptors is highly dependent on the specific (G α _q or G α ₁₃) untagged G α -subunit coexpressed (13), in this set of experiments, the BRET² signal in the absence of expression of the corresponding nontagged G α -subunit represents nonspecific binding. When GFP²-labeled G α -subunits were used, nonspecific binding was determined by substitution of the GFP²-G α with GABABR2-GFP². The BRET² signal from the receptor dimer/heterotrimeric G protein interaction was compared under basal and thrombin-induced activation conditions.

Interactions with G α _q were first probed by using GFP²- β ₁. Fig. 4A *Left* shows a significant agonist-dependent increase in BRET² signal for the PAR1/1 homodimer interaction with G α _qGFP²- β ₁ γ ₂. The same trend was observed for the PAR1/3 heterodimer.

Interactions with G α ₁₃ were then determined by using the same GFP²- β ₁ system. When G α ₁₃GFP²- β ₁ γ ₂ was used (Fig. 4A *Right*), the PAR1/1 homodimer showed an agonist-induced increase similar to that observed for G α _q. Strikingly, the PAR1/3 heterodimer showed a G α ₁₃ interaction in nonstimulated cells (to the level seen in stimulated PAR1/1 homodimer), which also showed a further agonist-induced increase.

The G α _q counterpart experiments using the GFP²-G α _q β ₁ γ ₂ G protein (Fig. 4B *Left*) yielded no significant agonist-induced changes for either the PAR1/1 or PAR1/3 dimer. However, the G α ₁₃ counterpart experiments using the GFP²-G α ₁₃ β ₁ γ ₂ G protein (Fig. 4B *Right*) showed an agonist-induced change in BRET² signal only in the PAR1/3 heterodimer and not in the PAR1/1. The trend was opposite that observed where the GFP² was placed on the G β ₁ subunit; i.e., here, an elevated BRET² signal was observed in nonstimulated cells, which decreased to nonspecific binding levels upon thrombin addition. Thus, PAR1/1 homodimer is capable of interacting with both G α _q and G α ₁₃, whereas PAR1 interacting with PAR3 alters its G α ₁₃ but not G α _q binding conformation.

We next determined whether the cleavage of PAR3 in the heterodimer contributed to the thrombin-induced-changes in G α ₁₃ binding conformation. Fig. 4B shows substitution of a thrombin-insensitive PAR3 mutant (T39P) (18) for the wild type had no effect. Thus, cleavage of PAR1 and not of PAR3 in the PAR1/3 heterodimer is sufficient to induce signal transduction.

Discussion

Our study focuses on the crucial role of PAR3 in regulating PAR1 function. We show that PAR1/3 heterodimers are formed constitutively and the activated dimeric complex induces distinct signaling involving the selective coupling to G α ₁₃ as compared with the PAR1/1 homodimer. Importantly, PAR1 has the ability to form heterodimers with PAR3, indicating that this heterodimer is readily formed under physiological conditions. Our findings are based on a differential BRET² signal using different combinations of PAR1 and PAR3 as well as receptor dimers

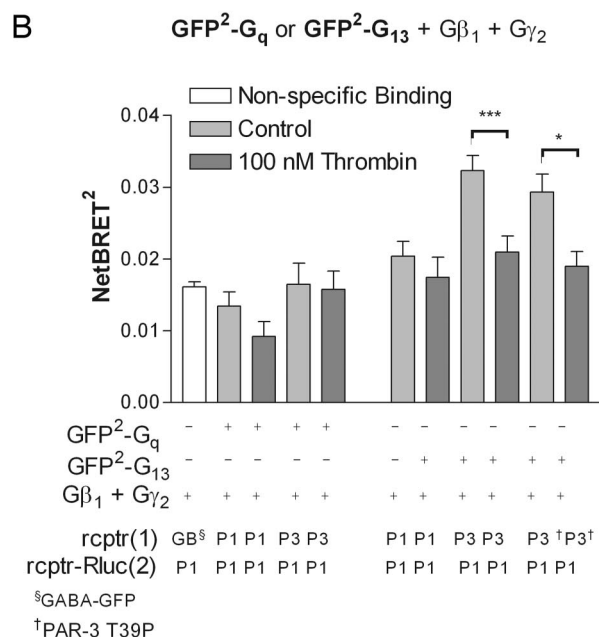
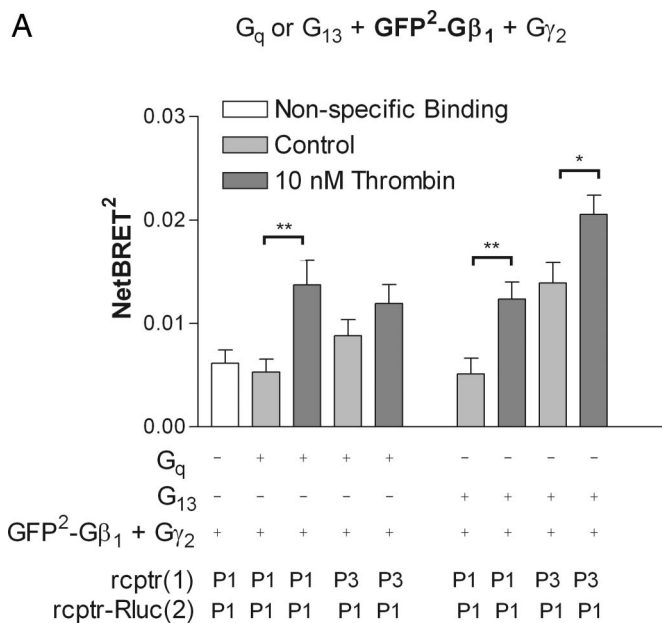


Fig. 4. PAR1 and PAR3 dimer composition is a determinant of agonist-induced changes in G protein coupling. PAR1-Rluc was transiently coexpressed in HEK293T cells with either nontagged PAR1 or nontagged PAR3, as indicated, to create specific receptor dimers. GFP^2 -labeled G proteins were introduced by expressing each subunit of the heterotrimer with either the $G\beta$ -subunit (A) or the $G\alpha$ -subunit (B) tagged with GFP^2 . BRET² signal due to nonspecific binding (white bars) was determined in the absence of expression of the corresponding nontagged $G\alpha$ -subunit (A) or by substitution of the corresponding GFP^2 - $G\alpha$ with GABABR2- GFP^2 (B). BRET² signal between receptor dimers and heterotrimeric G proteins under basal conditions (gray bars) was then compared with that under thrombin-induced activation (black bars). In B, a nontagged T39P, was also used where indicated. Each bar represents the average of at least three separate experiments performed in duplicate. Error bars represent \pm SEM. * and **, $P < 0.05$ and 0.01 , respectively.

together with different combinations of G protein subtypes. In addition, we used PAR knockdown by siRNA in endothelial cells to demonstrate that PAR3 regulates PAR1-mediated increase in endothelial permeability such that the PAR1/3 heterodimer

favors signaling through $G\alpha_{13}$ to mediate the permeability response.

The role of PAR3 is of interest, because the function of this apparently nonsignaling receptor remains obscure (18–20). The ability of PAR3 to generate intracellular signal also remains in doubt, because it lacks the cytoplasmic tail domain shown in other PARs to couple with G-proteins (18). In mouse platelets, PAR3 was shown to function as a cofactor of PAR4 by presenting thrombin to low-affinity PAR4, thereby resulting in efficient receptor cleavage (21). We show here that PAR3 directly interacts with PAR1 in endothelial cells to alter the PAR1/ $G\alpha_{13}$ binding conformation and thus induce activation of downstream signaling pathways distinct from activation of the PAR1/1 homodimer.

Several models of PAR trans- and coactivation have been proposed (11, 21–25). Studies showed that platelet-specific PAR1/4 heterodimerization was responsible for thrombin-induced platelet aggregation (26). Our results using BRET² demonstrated that PAR1 and PAR3 form highly specific homo- and heterodimer pairs in endothelial cells. The affinity of PAR1/3 interaction determined by BRET₅₀ was comparable to that of PAR1/1 homodimer. Thus, it is likely that a significant portion of PAR1 is complexed with PAR3 under physiological conditions in vascular endothelial cells.

A limitation in interpreting BRET data is that BRET relies on photon emission of Rluc as a catalytic byproduct of substrate hydrolysis. The weak BRET signal (compared with FRET) is difficult to detect microscopically. To circumvent this concern, we showed using confocal microscopy and immunohistochemistry that the receptor constructs used were indeed localized appropriately on the plasma membrane.

The ability of PAR1 and PAR3 to form homo- as well as heterodimers is likely due to their high sequence homology suggesting they share a conserved over-lapping dimerization interface. We demonstrated that dimerization pairing of PAR1 altered signaling; however, importantly, there was no evidence that PAR3 directly participated in either receptor dimer cleavage and activation or G protein activation.

The PAR1/3 heterodimer also showed differences in receptor desensitization compared with the PAR1/1 homodimer. TK stimulation had no effect on the PAR1/1 BRET signal but within 15–30 min caused a reduction in PAR1/3 signal. We infer from this finding that the differential effects of TK were due to differences in desensitization between the PAR1/1 and PAR1/3 dimer pairs. As activation of receptors by TK showed desensitization only in the presence of PAR3, this further supports our contention that the PAR1/3 heterodimer has a unique signaling property distinct from PAR1/1 homodimer.

We addressed the effects of PAR1/3 heterodimerization on PAR1 G protein specificity. We observed that PAR1/1 homodimers interacted with both $G\alpha_q$ and $G\alpha_{13}$ G proteins in an agonist-dependent manner. This finding is consistent with known interactions of PAR1 with G proteins (27, 28). However, we observed $G\alpha_q$ interactions using BRET² only when the GFP^2 label was placed on the $G\beta_1$ subunit. Given the geometric constraints of the assay, the GFP^2 expressed within the $G\alpha$ -subunit may not have been within the 100-Å limitation for efficient energy transfer from the receptor. There were similar $G\alpha_q$ interactions for the PAR1/3 heterodimer as the PAR1/1 homodimer, which we interpret to mean that dimerization with PAR3 has little effect on PAR1-mediated $G\alpha_q$ activation. However, the presence of PAR3 in the receptor pair markedly increased the interaction of PAR1 with $G\alpha_{13}$. Probing for $G\alpha_{13}$ interaction using the fluorescent $G\beta_1$ revealed that $G\alpha_{13}$ bound with the PAR1/3 dimer in the basal state but not with PAR1/1 dimer. $G\alpha_{13}$ coupling with PAR1/3 was further enhanced after stimulation with PAR1 agonist. In a related experiment using fluorescent $G\alpha_{13}$, we also showed that only the PAR1/3 heterodimer resulted in agonist-induced changes in

BRET² signal and unexpectedly, this change was opposite in direction (i.e., elevated BRET² signal in nonstimulated cells which decreased upon thrombin exposure). The opposite trend in BRET² depended on which subunit of the G protein was labeled. Thus, our results suggest upon agonist activation, conformational changes in the G protein enabled rotation of the N terminus of G β -subunit toward the C terminus of the receptor concomitant with a movement of the G α -subunit away from the C terminus of the receptor.

Our data demonstrate precoupling of the inactive PAR1/3 heterodimer with G α_{13} , which remains associated with the receptor heterodimer even after agonist activation of PAR1. This finding is consistent with studies of other GPCRs demonstrating unconventional receptor/G protein associations and kinetics (13). However, our findings contradict observations made in other systems that did not find precoupling of G-proteins with the receptor (29). We think that this discrepancy is likely due to different properties inherent in the G protein systems studied. Interestingly, precoupling to G α_{13} was only observed for the PAR1/3 heterodimer, indicating that PAR1 achieves the unique G α_{13} binding conformation only when PAR1 dimerized with PAR3.

The initial peak rise in thrombin-induced in [Ca²⁺]_i is attributed to release from intracellular Ca²⁺ stores as the result of activation of G α_q (30). Knockdown of PAR3 in endothelial cells using siRNA had no effect on the peak Ca²⁺ rise. This lack of effect suggests that PAR3 did not alter PAR1-G α_q binding. PAR1 knockdown altered both thrombin potency of the Ca²⁺ response, suggesting that thrombin signaling of the rise [Ca²⁺]_i was carried out primarily via the PAR1 subunit of the PAR1/3 heterodimer and formation of the heterodimer with PAR3 did not affect the PAR1-induced G α_q -mediated signaling.

The increase in endothelial permeability leading to vascular inflammation is the result of the integration of a network of signaling pathway dependent on G α_q as well as G α_{13} signaling (7–9). Changes in the activation of one or the other or both G-proteins (G α_q and G α_{13}) may affect the permeability response to thrombin. We observed that PAR1 knockdown markedly altered both thrombin's potency and efficacy, whereas PAR3 knockdown showed only a modest decrease in potency. These results demonstrate that thrombin signaling in endothelial cells is transmitted primarily by PAR1 cleavage but PAR1 interaction with PAR3 results in maximal activation of the PAR1-induced increase in endothelial permeability. The basis of this finding is that PAR3 dimerization with PAR1 changes the selectivity of PAR1 to G α_{13} , and thereby enhances G α_{13} -mediated signaling. Thus, PAR3 is a novel therapeutic target that may be useful in preventing vascular inflammation secondary increased endothelial permeability induced by thrombin.

Our data using a thrombin-insensitive mutant of PAR3 showed that cleavage of PAR1, and not of PAR3, in the PAR1/3 heterodimer complex is sufficient to induce signal transduction. These data support a pentameric complex formed from two GPCRs and one G protein, a model postulated for rhodopsin, the archetypal GPCR (31), and proposed for other GPCRs (32). In the case of rhodopsin, one receptor molecule serves as the photon (ligand) acceptor whereas the second serves as a platform to support G protein binding. Our data support the model for PARs in which one receptor (PAR1) is activated, and serves as the thrombin substrate, whereas the second receptor (PAR3) serves as an allosteric modulator to mediate G protein selectivity (Fig. 5).

In summary, we addressed regulation of endothelial cell signaling by PAR1/3 interaction and the crucial role of this interaction in determining G protein-coupling selectivity. We show an interaction of PAR3 with PAR1 that alters the PAR1/G α_{13} binding conformation. PAR1/1 homodimer is capable of interaction with G α_q and G α_{13} , whereas PAR1/3 heterodimer favors the G α_{13} binding conformation. PAR3 therefore functions as an important allosteric modulator of PAR1 signaling.

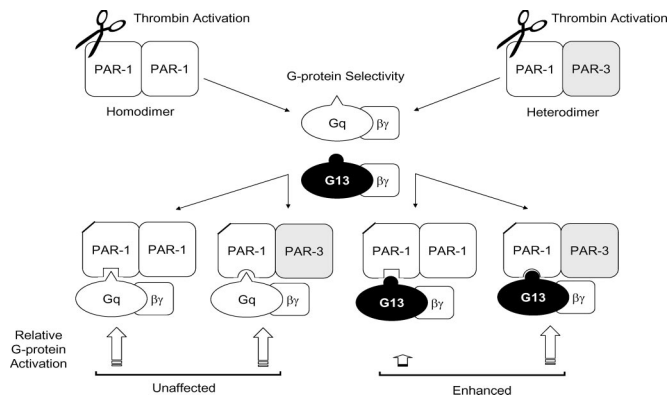


Fig. 5. PAR3 modulates PAR1 signaling by receptor dimerization. PARs are constitutively expressed as homo- and/or heterodimeric receptors. Protease induced activation of the PAR1 subunit of either the PAR1/1 homodimer or the PAR1/3 heterodimer initiates multiple intracellular signaling cascades by selective activation of discrete G-proteins. PAR1 heterodimerization with PAR3 alters the PAR1/G α_{13} binding conformation, enhancing G α_{13} signaling. Heterodimerization likely does not affect PAR1/G α_q selectivity.

Materials and Methods

Reagents. All cell culture reagents were purchased from Invitrogen (Carlsbad, CA), except endothelial growth medium-2 (EBM-2), which was obtained from Clonetics (San Diego, CA). α -Thrombin was purchased from Enzyme Research (South Bend, IN). TK was purchased from GL Biochem (Shanghai, China) Mouse anti-Rluc monoclonal antibody was purchased from Chemicon International (Temecula, CA). Alexa Fluor 594 rabbit anti-mouse IgG (H+L) was obtained from Molecular Probes (Eugene, OR). Human cDNA clones for PAR1, G α_q , G α_{13} , G β_1 , and G γ_2 in pcDNA3.1(+) were purchased from University of Missouri cDNA Resource Center, University of Missouri (Rolla, MO). The BRET² donor/acceptor fusion protein vectors pRluc-N and pGFP²-N were obtained from PerkinElmer (Boston, MA). All DNA primers, LipofectAMINE, TRIzol, and SuperScript III RT reagents were obtained from Invitrogen. siRNA was purchased from Dharmacon (Lafayette, CO). SYBR green PCR Master mix was purchased from Applied Biosystems (Branchburg, NJ).

Cell Culture. HPAECs were purchased from Cambrex (East Rutherford, NJ). Cells were maintained in EBM-2 medium supplemented with 10% FBS in 5% CO₂ at 37°C. All of the studies used cells between passages 5–8. HEK293T were maintained in DMEM supplemented with 10% FBS and penicillin/streptomycin (5,000 units/ml; 5,000 μ g/ml) in 5% CO₂ at 37°C.

cDNA Constructs. PAR1 and PAR3 were subcloned by PCR amplification into both the pRluc-N1 and pGFP²-N1 vectors (PerkinElmer). GFP² was amplified by PCR then inserted into G α_q in pcDNA3.1(+) between amino acid E119 and N120. The final protein sequence reads: M1... E119-EFGG-GFP²-GGEL-N120... stop. GFP² in G α_{13} in pcDNA3.1(+) final protein sequence reads: M1... P130-EFGG-GFP²-GGEL-M131... stop. GFP² was amplified by PCR and subcloned upstream of G β_1 in pcDNA3.1(+). A thrombin-insensitive mutant of PAR3 pcDNA3.1(+) was generated by mutating threonine 39 to a proline (18) by a PCR-based protocol. All constructs were verified by sequence analysis.

Transfections. HEK293T were grown in six-well plates to \approx 70% confluence. Between 0.5 and 2.5 μ g of each purified plasmid DNAs were incubated with 10 μ l of LipofectAMINE (Invitrogen) according to manufacturer's protocol. Cells were allowed to recover 48 h before experimentation.

Rluc Immunostaining and Confocal Microscopy. Subcellular localization of Rluc fusion proteins in HEK293T cells was determined by immunohistochemistry as described (33) using mouse anti-Rluc Ab (1:500) coupled with Alexa Fluor 594 rabbit anti-mouse IgG. Images were acquired with the Zeiss (Oberkochen, Germany) LSM 510 confocal microscope using a 63×1.2 N.A. water immersion objective.

BRET² Assay. BRET² assay was performed following the manufacturer's protocols (PerkinElmer). Briefly, HEK293T cells were grown in six-well plates and transiently transfected with fusion constructs of RlucGFP². After 48 h, cells were washed two times in PBS and detached by gentle pipetting. Media were removed by decanting after centrifugation at $1,000 \times g$ for 5 min, after which cells were resuspended in BRET buffer (PBS containing 1 mM MgCl₂, 1 mM CaCl₂, and 5 mM glucose) to a final density of $\approx 2.5 \times 10^6$ cells/ml. Cells were then stimulated with agonist as indicated just before addition of BRET² substrate DeepBlueC (PerkinElmer). BRET² signal was measured by using the Victor² (PerkinElmer) in luminescence mode by using bandpass filters for 410 and 515 nm. Values are reported as BRET² (absolute ratio of emission at 515 to emission at 410) or as NetBRET² (BRET²_{unknown} – BRET²_{background}), where BRET²_{background} is taken to be the BRET² signal obtained in the absence of an expressed GFP² acceptor protein. The absolute GFP² expression was measured by using the Victor² in fluorescence mode with excitation at 405 nm and emission at 515 nm. The absolute Rluc expression in the same cells was measured by using the Victor² in luminescence mode using no filters after addition of the non-BRET² substrate MightyLight (Novagen, San Diego, CA), according to the manufacturer's protocols.

siRNA Knockdown. HPAEC grown to confluence were harvested by detachment with 0.05% trypsin/0.5 mM EDTA followed by centrifugation, $1,000 \times g$ for 10 min at room temperature. Each reaction consisted of 1×10^6 cells resuspended in 100 μ l of basic nucleofector solution (Amaxa, Cologne, Germany) containing a

pool of three unique siRNA pairs for either PAR1 or PAR3 (0.25 nmol RNA each). Cells were then electroporated by using the Nucleofector Device according to manufacturer's protocols (Amaxa).

Semiquantitative RT-PCR. Expression of PAR1 and PAR3 was monitored in HPAEC by real-time semiquantitative RT-PCR by using PCR SYBR green PCR Master mix (Applied Biosystems) was on a PRISM 7000 Sequence Detection System (Applied Biosystems) with GAPDH as the internal control as described (34). Briefly, after siRNA treatment described above, HPAEC were grown to confluence in six-well plates and total RNA was harvested, reverse-transcribed using oligo-dTs with SuperScript III RT, and real-time semiquantitative analysis was performed. Data analysis and calculations were done following the $2^{-\Delta\Delta CT}$ method (35). Each sample was assayed in triplicate.

Calcium Mobilization. Calcium mobilization was determined as before (36). Briefly, after siRNA treatment, HPAEC were grown to confluence and serum deprived in EBM-2 containing 0.1% serum 3 h. Cells were then loaded with the FLIPR Calcium Plus kit dye and fluorescence measured on the FlexStation (Molecular Devices, Sunnyvale, CA).

TER. *In vitro* endothelial barrier dysfunction was monitored by electric cell-substrate impedance sensor (37). TER was determined as described (36). Briefly, after siRNA treatment, HPAEC were seeded at 2×10^5 cells/well and allowed to recover for 48 h. The monolayers were serum deprived in EBM-2 containing 0.1% serum 3 h before agonist addition.

We acknowledge the contributions of the following collaborators: Dr. Wadie F. Bahou (State University of New York, Stony Brook, NY) for the kind gift of the PAR3 construct; Dr. Michel Bouvier (Université de Montréal, Montréal, Canada) for assistance and the kind gift of the GABABR2-GFP² construct; Dr. Richard D. Minshall (University of Illinois, Chicago) for assistance in confocal microscopy; Dr. Tatyana Voynov-Yasenetskaya for direction in designing the GFP²-G α_{13} construct; and Dr. Shahid Siddiqui for design of the siRNA oligos.

- Malik AB, Fenton JW, 2nd (1992) *Semin Thromb Hemost* 18:193–199.
- Rabiet MJ, Plantier JL, Dejana E (1994) *Br Med Bull* 50:936–945.
- Cepkova M, Matthay MA (2006) *J Intensive Care Med* 21:119–143.
- Bastarache JA, Ware LB, Bernard GR (2006) *Semin Respir Crit Care Med* 27:365–376.
- Jenkins RG, Su X, Su G, Scotton CJ, Camerer E, Laurent GJ, Davis GE, Chambers RC, Matthay MA, Sheppard D (2006) *J Clin Invest* 116:1606–1614.
- Vu TK, Hung DT, Wheaton VI, Coughlin SR (1991) *Cell* 64:1057–1068.
- Dudek SM, Garcia JG (2001) *J Appl Physiol* 91:1487–1500.
- Hart MJ, Jiang X, Kozasa T, Roscoe W, Singer WD, Gilman AG, Sternweis PC, Bollag G, Sternweis PM, Sharma S, et al. (1998) *Science* 280:2112–2114.
- Tiruppathi C, Minshall RD, Paria BC, Vogel SM, Malik AB (2002) *Vascul Pharmacol* 39:173–185.
- Hirano K, Kanaide H (2003) *J Atheroscler Thromb* 10:211–225.
- O'Brien PJ, Prevost N, Molino M, Hollinger MK, Woolkalis MJ, Woulfe DS, Brass LF (2000) *J Biol Chem* 275:13502–13509.
- Pfleger KD, Eidne KA (2005) *Biochem J* 385:625–637.
- Gales C, Rebois RV, Hogue M, Trieu P, Breit A, Hebert TE, Bouvier M (2005) *Nat Methods* 2:177–184.
- Milligan G (2004) *Eur J Pharmacol Sci* 21:397–405.
- Pfleger KD, Eidne KA (2003) *Pituitary* 6:141–151.
- Mercier JF, Salahpour A, Angers S, Breit A, Bouvier M (2002) *J Biol Chem* 277:44925–44931.
- Hughes TE, Zhang H, Logothetis DE, Berlot CH (2001) *J Biol Chem* 276:4227–4235.
- Ishihara H, Connolly AJ, Zeng D, Kahn ML, Zheng YW, Timmons C, Tram T, Coughlin SR (1997) *Nature* 386:502–506.
- Hansen KK, Saifeddine M, Hollenberg MD (2004) *Immunology* 112:183–190.
- Kaufmann R, Schulze B, Krause G, Mayr LM, Settmacher U, Henklein P (2005) *Regul Pept* 125:61–66.
- Nakanishi-Matsui M, Zheng YW, Sulciner DJ, Weiss EJ, Ludeman MJ, Coughlin SR (2000) *Nature* 404:609–613.
- Chen J, Ishii M, Wang L, Ishii K, Coughlin SR (1994) *J Biol Chem* 269:16041–16045.
- Shi X, Gangadharan B, Brass LF, Ruf W, Mueller BM (2004) *Mol Cancer Res* 2:395–402.
- Vesey DA, Cheung CW, Kruger WA, Poronnik P, Gobe G, Johnson DW (2005) *Kidney Int* 67:1315–1329.
- Damiano BP, Cheung W-M, Santulli RJ, Fung-Leung W-P, Ngo K, Ye RD, Darrow AL, Derian CK, de Garavilla L, Andrade-Gordon P (1999) *J Pharmacol Exp Ther* 288:671–678.
- Leger AJ, Jacques SL, Badar J, Kaneider NC, Derian CK, Andrade-Gordon P, Covic L, Kuliopulos A (2006) *Circulation* 113:1244–1254.
- Hung DT, Wong YH, Vu TK, Coughlin SR (1992) *J Biol Chem* 267:20831–20834.
- Barr AJ, Brass LF, Manning DR (1997) *J Biol Chem* 272:2223–2229.
- Hein P, Frank M, Hoffmann C, Lohse MJ, Bunemann M (2005) *EMBO J* 24:4106–4114.
- Lum H, Aschner JL, Phillips PG, Fletcher PW, Malik AB (1992) *Am J Physiol* 263:L219–L225.
- Jastrzebska B, Fotiadis D, Jang G-F, Stenkamp RE, Engel A, Palczewski K (2006) *J Biol Chem* 281:11917–11922.
- Baneris JL, Parello J (2003) *J Mol Biol* 329:815–829.
- Sandoval R, Malik AB, Naqvi T, Mehta D, Tiruppathi C (2001) *Am J Physiol* 280:L239–L247.
- McLaughlin JN, Mazzoni MR, Cleator JH, Earls L, Perdigoto AL, Brooks JD, Muldowney JA, III, Vaughan DE, Hamm HE (2005) *J Biol Chem* 280:22172–22180.
- Livak KJ, Schmittgen TD (2001) *Methods* 25:402–408.
- McLaughlin JN, Shen L, Holinstat M, Brooks JD, Dibenedetto E, Hamm HE (2005) *J Biol Chem* 280:25048–25059.
- Tiruppathi C, Malik AB, Del Vecchio PJ, Keese CR, Giaever I (1992) *Proc Natl Acad Sci USA* 89:7919–7923.